



Defect structure and properties of Mg-Doped La Cr O_{3-δ}

Madoui Nadia^{*}, Mahmoud Omari

Departement de chimie, Université de Biskra, B.P.145, 07000 Biskra-Algeria.

Abstract

A defect chemical model for the behaviour of acceptor-doped LaCrO₃ as a function of oxygen pressure is proposed. This is considered within the regime that corresponds to oxygen deficit oxygen. The mathematical approach allows us to calculate the oxygen partial pressure dependant properties of LaCr_{1-x}Mg_xO_{3-δ} in the value(x= 0.05, 0.1, 0.2). The results show that the conductivity was independent of pO₂ and was proportional to the dopant concentration at high pO₂. Therefore, under reducing conditions, the conductivity decreased exponentially with decreasing pO₂ and asymptotically approached a pO₂^{1/4} relationship. Stability regimes and compensation mechanisms at various oxygen partial pressures and temperatures are proposed. This model also examines the charge compensation mechanisms that dominate under the different regimes and their implications for transport properties. From equilibrium constants, thermodynamic quantities such as standard enthalpy and entropy change for the defect formation reactions were calculated.

Keywords: Defect modelling, Perovskite, Conductivity.

PACS: 74.62.Dh, 78.67.Pt, 72.15.-v.

^{*}) For correspondence; Email: madouin@yahoo.fr.

1. Introduction

Solid oxide fuel cells (SOFCs) are environmentally clean and highly efficient devices used to generate electricity electrochemically. Limited by the oxygen conductivity of the electrolyte, the most widely studied zirconia-based SOFCs must operate at about 1000 °C. Such high operating temperatures cause electrode reaction and other engineering difficulties. Many efforts are still underway to find alternative electrolytes with higher conductivity at lower temperatures. Among these are studies that have been carried out on bismuth based mixed oxides such $\text{Bi}_2\text{O}_3\text{-Ln}_2\text{O}_3$ ($\text{Ln} = \text{La, Nd, Sm, Dy, Er, Yb}$)¹ and $\text{Bi}_2\text{O}_3\text{-Sm}_2\text{O}_3\text{-V}_2\text{O}_5\text{-MO}$ ($\text{M} = \text{Pb, Ni, Co}$)². The perovskite-type oxide solid solutions a series of La-doped SrTiO_3 and Mg doped LaCrO_3 (O-20 at. %) compounds were prepared by the liquid mix process³. In all cases stoichiometric A/B ratio was maintained, i.e., $(\text{Sr} + \text{La})/\text{Ti}$ or $\text{La}/(\text{Cr} + \text{Mg}) = 1$.

Lanthanum chromite, on the other hand, is known to be a p-type oxide⁴ and becomes non-stoichiometric through the formation of cation vacancies. It is one of the promising materials for high temperature electrode applications and fuel cell interconnects⁵; however, volatilization and possibly corrosion impose certain limitations on the use of LaCrO_3 . Several studies have been reported⁶ relating its chemical stability and cation stoichiometry to volatilization and electrical conductivity.

$\text{LaCr}_{1-x}\text{Mg}_x\text{O}_{3-\delta}$ have been extensively studied due to their potential application as an air electrode in high-temperature oxide fuel cells, chemical sensor elements and electrodes for magneto hydrodynamic (MHD) generators, because some of them show high catalytic activity. Several useful properties of these perovskite type oxides such as electrical conductivity and electron emission are the result of their non-stoichiometry and electronic structure. Partial replacement of chromium by magnesium leads to increased electronic disorder and to changes in the oxidation state of the 3d transition metal and in the oxygen non-stoichiometry.

The properties of the perovskite-type oxide are generally quite sensitive to oxygen deficiency and B-site composition. In spite of the importance of oxygen non-stoichiometry, limited studies have been performed, so far, on the non-stoichiometry and the related defect structure of $\text{LaCr}_{1-x}\text{Mg}_x\text{O}_{3-\delta}$. Anderson et al. measured the non-stoichiometry for the $\text{LaCr}_{1-x}\text{Mg}_x\text{O}_{3-\delta}$

($x = 0.05, 0.1, \text{ and } 0.2$) as a function of temperature, T , and oxygen partial pressure, pO_2 . Anderson et al. suggested that the conductivity of $LaCr_{0.9}Mg_{0.1}O_{3-\delta}$ arises from the presence of multivalent Cr ions due to Mg doping [8]. For these purposes, the conduction behaviour under low oxygen pressures must be investigated, since if an appreciable electronic conduction arises as a result of defect equilibrium at low pO_2 its electrical conduction is determined by the concentration of present defects in the system. Several years ago, Spinolo et al. suggested a general mathematical method to calculate defect concentrations but without application to actual oxides^{9, 10}. Recently, Poulsen proposed a defect model for calculating defect concentrations in proton containing perovskites¹¹ and LCM³ within a wide range of partial pressure of oxygen.

The purpose of the present work is to establish defect model equilibrium of $LaCr_{1-x}Mg_xO_{3-\delta}$ for the value ($x = 0.05, 0.10, 0.20$) using the nonstoichiometry data that were reported by Anderson et al. [7]. The present defect model will allow us to interpret the thermo gravimetric results in which oxygen vacancies are assumed for the oxygen deficient condition. The relationship between the obtained results and those of conductivity measurements [8],[12] will also be discussed. Finally, from equilibrium constants, thermodynamic quantities such as standard enthalpy and entropy change for the defect formation reactions are calculated.

2. Defect Chemical Model

The defect model proposed here is considered within the regime that corresponds to oxygen deficit oxygen. Only 1 sublattice of $LaCr_{1-x}Mg_xO_{3-\delta}$ is assumed to be defected. Reduction of this system leads to an oxygen deficit in the oxygen sublattice. Interactions between defects and interstitial oxygen are neglected. This model is a random point defect model, based on the presence of 2 oxidation states of chromium Cr (Cr^{4+}) and Cr^x (Cr^{3+}) that are populated in various proportions depending on temperature, partial pressure of oxygen and Mg doping.

It does not take into account activity coefficients of all present species. The oxygen non-stoichiometry assumes negative values, which is explained by the presence of oxide ion vacancies. In the point defect model, the oxygen vacancies are assumed to be fully

ionized at high temperatures. In common with earlier work¹³⁻¹⁶, this treatment ignores the Schottky defect equilibrium for which, in any case, the equilibrium constant is not available.

For the treatment of point defects in this system we chose the "Kröger-Vink notation"¹⁷. We therefore define vacancies as particles that occupy a defined site in a crystal and that may have a charge. Sites in a crystal are the points where the atoms or the vacancies may be. For a crystal composed of 2 kinds of atoms we have, for example, the "cationic-sites" and the "oxygen-sites". A point, a negative charge, marks the positive excess charge by a dash to distinguish this relative charge from the absolute charge.

Adopting this type of notation we obtain on the whole a set of independent equations containing the 3 concentrations of the different species (Table 1), these are

Table 1: Different species used in this defect model with Kröger-Vink notation.

Cation site	Anionic site
Cr (Cr ⁴⁺)	O _o ^x
Cr ^x (Cr ³⁺)	V _o ^{..}
Mg [!] (Mg ²⁺)	

- The charge-neutrality condition leads to

$$2(V^{\cdot\cdot}o) + (Cr^{\cdot}) = (Mg^!) \tag{1}$$

- The value of (Mg[!]) is given by the nominal B -site composition x.
That is

$$(Mg^!) = x \tag{2}$$

Because this solid solution is an oxygen deficient type, we have

$$(V^{\cdot\cdot}o) = \delta \tag{3}$$

From equations (1)-(3), we have:

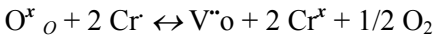
$$x = 2 \delta + (Cr^{\cdot}) \quad (4)$$

With decreasing pO_2 , (Cr^{\cdot}) becomes sufficiently low so that

$$x \approx 2 \delta \quad (5)$$

Where in Kröger-Vink notation Mg^{\cdot} and Cr^{\cdot} denote, respectively, the Mg^{2+} and Cr^{4+} cations on a Cr^{3+} lattice position.

- Reaction redox leading to oxygen vacancies



Oxygen vacancies $V^{\cdot\cdot}o$ are formed and Cr^{4+} (Cr^{\cdot}) cations are reduced to Cr^{3+} (Cr^x) at low oxygen partial pressures.

$$K_{ox} = (V^{\cdot\cdot}o) (Cr^x)^2 pO_2^{1/2} / [(O^x)(Cr^{\cdot})^2] \quad (6)$$

In order to maintain the fixed A/ B ratio, the following equation must be maintained:

$$(Cr^{\cdot}) + (Cr^x) = 1 \quad (7)$$

Kröger-Vink notation¹⁷ is used with La (+3) Cr (+3) O₃ as the reference state.

The experimental non-stoichiometry data as a function of pO_2 are fitted to equation (6) taking the equilibrium constant as a fitting parameter.

$(V^{\cdot\cdot}o)$: test value in the interval 10^{-10} to 0.5. The step-wise calculation proceeds as follows:

We assume a value for $(V^{\cdot\cdot}o)$

$$(O^x_o) = 3 - (V^{\cdot\cdot}o) \quad (8)$$

From equation (7) we obtain

$$(Cr^{\cdot}) = 1 - (Cr^{x}) \quad (9)$$

By substituting (Cr^{\cdot}) in equation (4) one obtains the following expression:

$$(Cr^{x}) = 1 + 2\delta - x \quad (10)$$

If the set of concentrations are accepted, we can insert $(V^{\cdot\cdot o})$, $(O^x o)$, (Cr^x) and (Cr^{\cdot}) into equation (6) and find the oxygen partial pressure that corresponds to the equilibrium concentrations. The calculation is next performed for a new value of $(V^{\cdot\cdot o})$ until all the concentration interval of interest has been covered

3. Results and Discussion

The simulations are normally made for an interval $(V^{\cdot\cdot o})$ from an arbitrarily chosen lowest limit of $10^{-10.5}$ up to 0.5. Solutions are normally generated for a very wide pO_2 span from 10^{-11} to 1 atm. Calculation and plotting of all concentrations at different pO_2 s are carried out on a Pentium IV. The equilibrium constants used in the following are calculated using non-stoichiometric values TG-data⁷.

4. Defect concentration in $LaCr_{1-x}Mg_xO_{3-\delta}$

For the comparison, we chose to present for all species and in the same defect diagram their concentrations as a function of pO_2 . Figure 1 shows the defect diagram for LSC10 with all kinds of vacancies and metal. It can be easily seen from the plot that for $pO_2 > 10^{-11}$ atm the predominant ions are Cr^{3+} . There are no physical solutions for the set of 3 concentrations at $pO_2 < 10^{-11}$ atm where (Cr^{\cdot}) concentration goes negative, i.e. all chromium is in oxidation state +3, at $O \text{ total} / Cr \approx 2.5$.

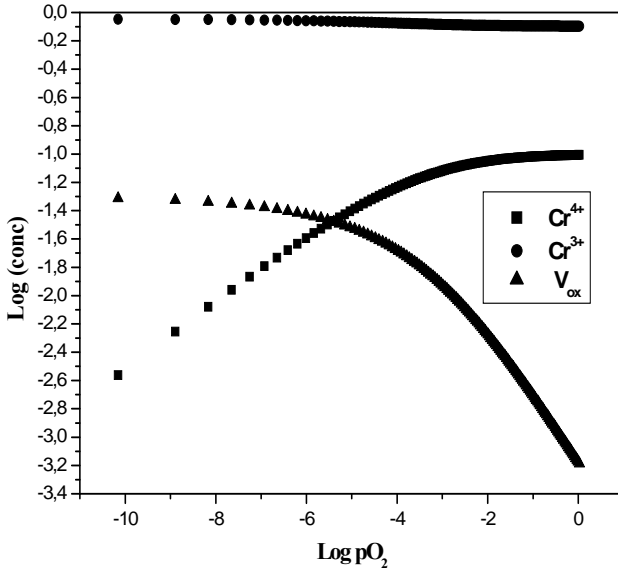


Fig: 1 Defect diagram for LCM10 at 1304°C

The relative carrier concentration for LCM10 as a function of pressure at different temperatures is shown in Figure 2. The variation of (Cr^{\cdot}) for $LaCr_{0.9}Mg_{0.1}O_3$ as a function of partial pressure calculated by H.U. Anderson et al.¹⁸ is similar to the obtained results (Figure 1) for LCM10. In the ionic compensation charge, the carrier concentration appears to be in agreement with pO_2 dependence proposed by the model within the temperature range investigated (1116°C, 1200°C, 1304°C, 1368°C). As expected, the figure further indicates that, in the intermediate pO_2 range, where electronic compensation predominates, the carrier concentration is independent of both temperature and pO_2 . The transition from pO_2 dependence to independence shifts to higher oxygen partial pressure as the temperature of equilibration increases from 1116°C, 1200°C, 1304°C, 1368°C. A plot of log carrier concentration as a function of $pO_2^{1/4}$ is expected to be linear in the region where ionic compensation is predominant. Critical pO_2 corresponding to the reduction and the oxidation of chromium shifted to higher pO_2 when the temperature

increased. At $pO_2 > 10^{-8}$ atm, $\log(Cr^{4+})$ is practically constant and equal to -1. The concentration dependence with pO_2 at low and high values of partial pressure is similar to that of LCM³.

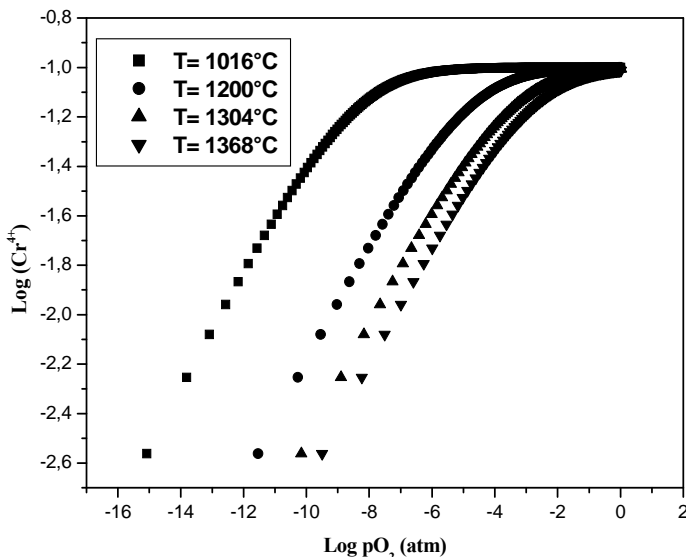


Fig. 2: Relative carrier concentration as a function of pO_2 and temperature for LCM10.

The effect of Mg content at 1304 °C on the carrier concentration is shown in Figure 3. The relative carrier concentration appears to have a one-fourth power dependence on pO_2 in the region where oxygen compensation is expected ($pO_2 < 10^{-2}$ atm). The Figure also indicates that the transition from ionic to electronic compensation occurs at relatively higher pO_2 as the Mg content increases, as expected from the model. The calculated nonstoichiometry as a function of pO_2 for LCM5, LCM10 and LCM20 at 1304°C is presented in Figure 4. When magnesium content, at lower pO_2 , the amount of oxygen non-stoichiometry reaches the limit $\delta = (x/2)$ as predicted from equation (4). This plateau corresponds to a new stoichiometric state where all chromium is in Cr^{3+} . Oxygen vacancy

begins to form at 10^{-8} to 10^{-6} atm of pO_2 . The calculated non-stoichiometry Isotherms are in good agreement with the reported thermogravimetry data³ and similar to those obtained for Mg doped $LaCrO_3$ ¹⁹. These results conform very well to those obtained for the dependence of carrier concentration with pO_2 (Figure 3).

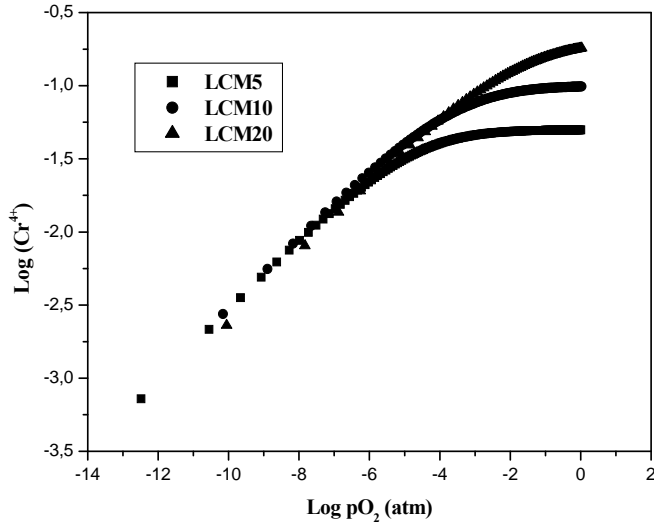


Fig.3: Relative carrier concentration as a function of pO_2 and composition at $1304C^\circ$ for LCM5, LCM10, LCM20

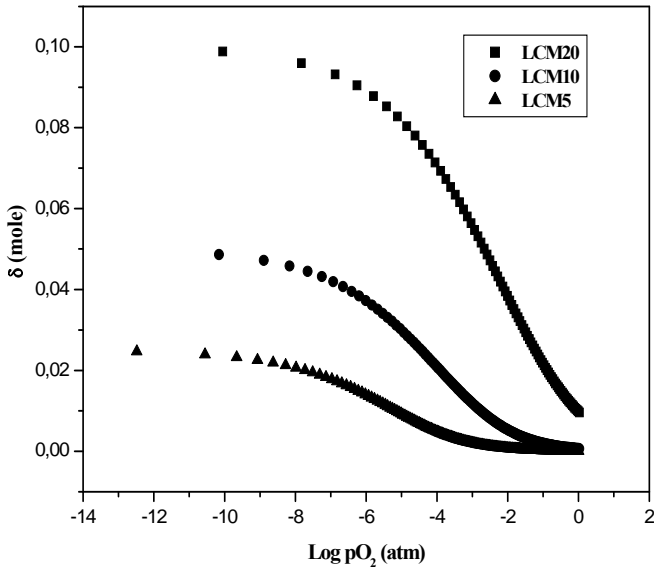


Fig. 4: Simulated oxygen nonstoichiometry at 1304°C for 3 different compositions, LCM5, LCM10 and LCM20

The effect of temperature on oxygen non-stoichiometry of LCM10 is shown in Figure 5. At higher temperatures, oxygen vacancies begin to form at higher pO_2 (10^{-11} to 10^{-6} atm) and their amounts approach the constant values at lower pO_2 (10^{-1} atm), which corresponds to a new stoichiometric state. In this case also, we see a good agreement between these results and those concerning the effect of temperature on the relative carrier concentration (Figure 2). This behavior is the same as that was found in Mg - doped $LaCrO_3$ ¹⁹ . The critical pO_2 range corresponding at the transition from the ionic to the electronic compensation charge is practically the same (10^{-13} to 10^{-6} atm).

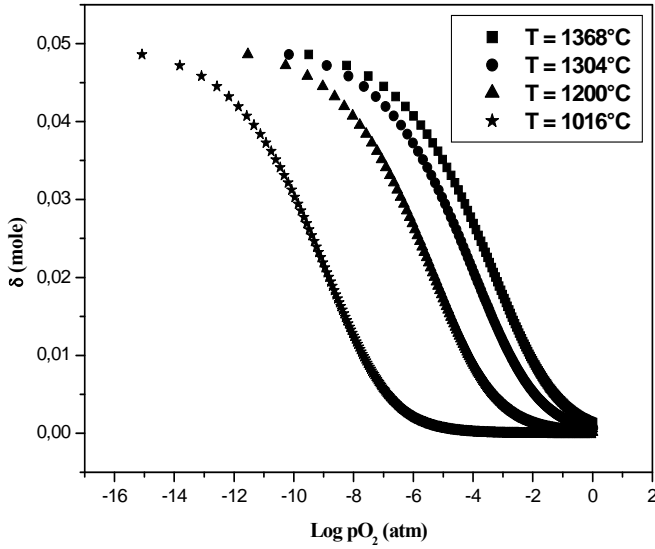
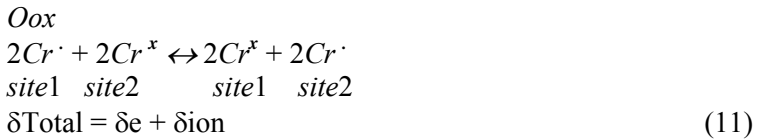


Fig. 5: Simulated oxygen nonstoichiometry of LCM10 as a function of oxygen partial pressure at 4 different temperatures.

5. Electrical Conductivity

Total conductivity is the summation of the individual contributions from ionic and electronic carriers. Each term is a product of the numerical value of the charge of the carrier, the relative concentration of the carrier and the kind of mobility for that carrier. The electron transport can be formulated as a charge transfer reaction as follows:



Poulsen⁷ has proposed an expression of total conductivity as a function of different concentration species.

$$\delta_{\text{total}} = m_e(\text{Cr}^{\cdot}) + m_{\text{ion}} / - 2 / (\text{O}^{\times}_{\text{o}})(\text{V}^{\cdot\cdot}_{\text{o}}) \quad (12)$$

Where m_e and m_{ion} represent electronic and ionic mobility respectively.

Figure 6 presents the dependence of conductivities on oxygen partial pressure as a function of composition at 1304°C. All compositions showed common characteristics:

- Little $p\text{O}_2$ dependence was observed in a range of high $p\text{O}_2$ and this range narrows with increasing temperature. As reduction proceeded, the electrical conductivity decreased with approximately $p\text{O}_2^{1/4}$. An abrupt decrease in electrical conductivity occurred under high reducing conditions.
- The critical $p\text{O}_2$ shifted to higher $p\text{O}_2$ when the temperature and / or the dopant concentration were increased.

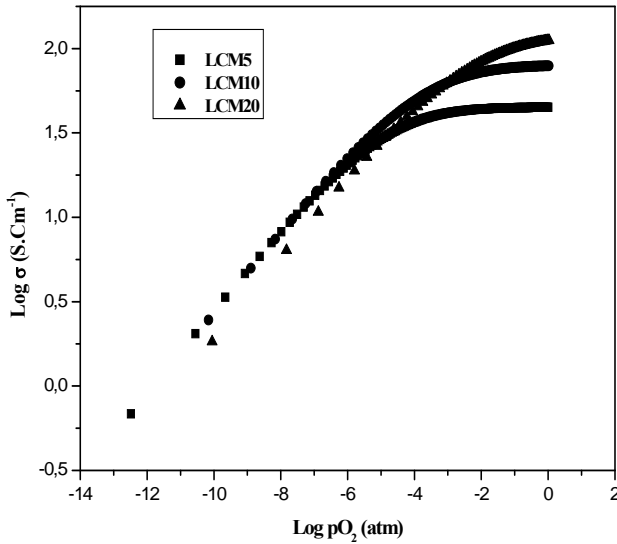


Fig. 6: Conductivity isotherms at 1304°C for three different compositions LCM5, LCM10 and LCM20

The electrical conductivity appears to have a one-fourth power dependence on the oxygen partial pressure in the region (10^{-14} to 10^{-2} atm). The figures also indicate that the transition from ionic to electronic compensation occurs at relatively higher pO_2 as the Mg content increases, as expected from the model. The effect of temperature on the conductivity for LCM10 is shown in Figure 7. In the ionic compensation region, the electrical conductivity dependence on oxygen partial pressure proposed by this model is in good agreement with Meadowcroft's work¹². This behaviour is similar to that observed in Mg-doped $LaCrO_3$ ^{19; 20} and LCM³. As expected, the figure further indicates that, in the intermediate pO_2 range, where electronic compensation predominates, the conductivity is independent of both temperature and pO_2 . The transition from pO_2 dependence to independence shifts to higher oxygen partial pressure as the temperature of equilibration increases from (1116°C, 1200°C, 1304°C and 1368°C). These results are in close agreement with the reported conductivity measurements^{8; 12}.

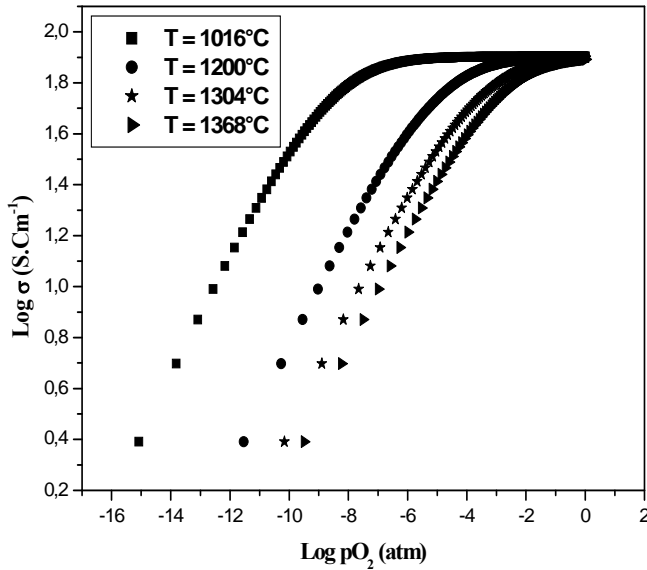


Fig. 7: Electrical conductivity of $\text{LaCr}_{1-x}\text{Mg}_x\text{O}_{3-\delta}$ as a function of pO_2 at 4 temperatures.

The conductivity at high pO_2 has a weak pO_2 dependence, the product $(\text{Cr}^\cdot)(\text{Cr}^x)$ is constant until 10^{-8}atm and the conductivity decreases with an approximate slope $\partial(\log\sigma) / \partial(\log\text{pO}_2) \approx 0.4$. This is in accordance with the experiments^{8; 12}. Anderson et al. suggested that $\text{LaCr}_{0.9}\text{Mg}_{0.1}\text{O}_{3-\delta}$ is a p-type conductor and its conductivity arises from the presence of multivalent Cr ions due to Mg doping⁸. The constant electrical conductivity that exists in the high pO_2 region may be easily understood if it is assumed that acceptors control the carrier concentration and that the electronic compensation predominates. In the lower pO_2 region, oxygen vacancies are formed and the electrical conductivity begins to decrease due to ionic charge compensation. The conductivity mechanism in acceptor-doped lanthanum chromites is due, as mentioned in the literature, to small - polaron hopping irrespective of the kinds of dopants^{19, 20}.

6. Thermodynamic considerations of the defect model

Some useful thermodynamic quantities such as ΔG°_{ox} , the standard free energy change, ΔS°_{ox} the standard entropy and ΔH°_{ox} the standard enthalpy change for the reaction of equation (6) can be easily calculated according the following equations:

$$\Delta G^{\circ}_{ox} = -RT \ln K_{ox} = \Delta H^{\circ}_{ox} - T\Delta S^{\circ}_{ox} \quad (13)$$

$$\Delta S^{\circ}_{ox} = -\partial (\Delta G^{\circ}_{ox})/\partial T \quad (14)$$

And

$$\Delta H^{\circ}_{ox} = \Delta G^{\circ}_{ox} + T\Delta S^{\circ}_{ox} \quad (15)$$

These quantities are calculated for LCM10 using the equilibrium constants (Table 2) by the least-squares method and are shown in Tables 3 and 4. The enthalpy of the reaction was obtained from the slope of the Arrhenius plot. The ΔS°_{ox} values depend on the composition x and are relatively close to those obtained for $\text{LaCr}_{1-x}\text{Mg}_x\text{O}_{3-\delta}$ ²³. The slight difference from values of ΔH°_{ox} and ΔS°_{ox} for the same Mg - doped LaCrO_3 is due to interactions between defects that we do not take into account in the present defect model. The changes in standard enthalpy and standard entropy show composition dependence with acceptor-dopant. These were estimated to be - 33.63 Kcal/mol and - 17.61 cal.mol⁻¹.K⁻¹ for $\text{LaCr}_{0.9}\text{Mg}_{0.1}\text{O}_{3-\delta}$. From these results, the standard enthalpy depends strongly on composition, so the ideal solution approximation cannot be applied to the Mg concentration change. This behavior was also suggested for $\text{LaCr}_{1-x}\text{Mg}_x\text{O}_{3-\delta}$ by Anderson⁴, which is in good agreement with the non-stoichiometry data^{19, 20}.

Table 2. Equilibrium constants for LCM10

composition	T (°C)	K _{ox}
LCM10	1016	5,09 10 ⁻⁵
	1200	3 10 ⁻³
	1304	1,47 10 ⁻²
	1368	3,15 10 ⁻²
LCM5	1304	8,22 10 ⁻²
LCM20	1304	3,88 10 ⁻²

Table 3. Standard enthalpy and entropy change for the formation of oxygen vacancies.

Composition : LCM10	ΔH°_{ox} (Kcal/mol)	ΔS°_{ox} (cal.mol ⁻¹ .K ⁻¹)
La Cr _{0.9} Mg _{0.1} O _{3-δ}	- 33.63	- 17.61

Table 4: Standard free energy change for the formation of oxygen vacancies for LCM10.

T (°C)	T (K)	$\Delta G^{\circ}_{ox} = - RT \text{ Log } k_{ox}$ (Kcal/mol)	$\Delta G^{\circ}_{ox} = \Delta H^{\circ}_{ox} - T\Delta S^{\circ}_{ox}$
1016	1289	-11,07	$\Delta S^{\circ}_{ox} = - 17.61$ (cal/mol.k)
1200	1473	-7,43	
1304	1577	-5,78	$\Delta H^{\circ}_{ox} = - 33.63$ (kcal/mol)
1368	1641	-4,93	

7. Conclusion

The data obtained from TG experiments support the proposed defect model for the oxidation behavior of acceptor-doped LaCrO_3 . This defect model indicates that at high $p\text{O}_2$ electronic compensation occurs by a transition of Cr^{3+} to Cr^{4+} , whereas ionic compensation takes place at lower $p\text{O}_2$ by the formation of oxygen vacancies. The oxygen partial pressure at which electronic compensation shifts to ionic is both acceptor dopant and temperature dependent. The general behaviour is that the transition shifts to higher oxygen partial pressure as the temperature or the concentration of acceptor-dopant increases. The phase stability of Mg-doped LaCrO_3 against reduction was shifted to higher $p\text{O}_2$ when the temperature and / or Mg-dopant concentrations increased. The changes in standard enthalpy and standard entropy show composition dependence with acceptor-dopant. They were estimated to be -33.63 Kcal/mol , $-17.61 \text{ cal.mol}^{-1}.\text{K}^{-1}$ for $\text{LaCr}_{0.9}\text{Mg}_{0.1}\text{O}_{3-\delta}$.

References

- [1] H. Iwahara, T. Esaka, T. Sato, *J. Solid State Chem.*, **39** (1981) 173
- [2] M. Benkaddour, M. Omari, J. C. Boivin, P. Conflant, M. Drache, *Ann. Chim. Sci. Mat.* **25** (2000) 165
- [3] F. W. Poulsen, *Solid State Ionics*, **129** (2000) 145
- [4] D. B. Meadowcraft, in "Proceedings, Int. Conf. on Strontium-Containing Compounds" (T. Gray, Ed.), Atlantic Res. Inst., Halifax, N. S. (1973) **119**
- [5] J. H. Kuo, H. U. Anderson, D. M. Sparlin, *Solid State Chemistry* **83** (1989) 52
- [6] D. B. Meadowcraft, J. M. Wimmer, *Ceram. BUN.* **58** (1979) 610
- [7] D. B. Meadowcraft, *Brit. J. Appl. Phys.* **2**, 1225 (1969)
- [8] H. U. Anderson, "Conference of High Temperature Sciences Related to Open Cycle, Cool-fired MHD Systems," Argonne National Laboratory, April 4-6, 1977, Argonne, Ill.
- [9] D. B. Meadowcraft, *Br. J. Appl. Phys.* **2** (1969) 1225
- [10] G. Spinolo, U. Anselmi-Tamburini, *Ber. Bunsenges. Phys. Chem.*, **99**, (1995) 87

- [11] G. Spinolo, U. Anselmi-Tamburini, P. Ghigna, Z. Für Naturforschung, A **52** (1997) 629
- [12] F. W. Poulsen, J. Solid State Chem., **143** (1999) 115
- [13] D. B. Meadowcroft, Br. J. Appl. Phys., **9** (1969) 1225
- [14] H. Uchida, H. Yoshikawa, H. Iwahara, Solid State Ionics, **35** (1989) 229
- [15] Y. Larring, T. Norby, Solid State Ionics, **97**, (1997) 523
- [16] T. Schober, H. Wenzl, Ionics, **81**, (1995) 111
- [17] T. Schober, W. Schilling, H. Wenzl, Solid State Ionics, **86** (1996) 653
- [18] F. A. Kröger, H.J. Vink, Solid State Physics, Vol. **3** (1956) 307
- [19] B. A. Van Hassel, T. Kawada, N. Sakai, H. Yokokawa, M. Dokiya, H. J. M. Bouwmeester Solid State Ionics, **66** (1993) 295
- [20] H. U. Anderson, M. M. Nasrallah, B. K. Flandermeyer, A. K. Agarwal, J. Sol. Stat. Chem. **56** (1985) 325
- [21] B. K. Flandermeyer, M. M. Nasrallah, A. K. Agarwal, H. U. Anderson, J. Amer. Ceram. Soc. **67** (1984) 195
- [22] D. P. Karim, A. T. Aldred, Phys. Rev. B, **20** (1979) 1255
- [23] J. B. Webb, M. Sayer, A. Mansingh, Can. J. Phys., **55** (1977) 1725
- [24] S. Tanasescu, N. D. Totir, D. Neiner, J. Optoelectronic and Advan. Mater. vol. **3** (2001) 101